

Nanoscale

Accepted Manuscript



This is an *Accepted Manuscript*, which has been through the Royal Society of Chemistry peer review process and has been accepted for publication.

Accepted Manuscripts are published online shortly after acceptance, before technical editing, formatting and proof reading. Using this free service, authors can make their results available to the community, in citable form, before we publish the edited article. We will replace this *Accepted Manuscript* with the edited and formatted *Advance Article* as soon as it is available.

You can find more information about *Accepted Manuscripts* in the [Information for Authors](#).

Please note that technical editing may introduce minor changes to the text and/or graphics, which may alter content. The journal's standard [Terms & Conditions](#) and the [Ethical guidelines](#) still apply. In no event shall the Royal Society of Chemistry be held responsible for any errors or omissions in this *Accepted Manuscript* or any consequences arising from the use of any information it contains.

Cite this: DOI: 10.1039/c0xx00000x

www.rsc.org/xxxxxx

ARTICLE TYPE

Switchable Supramolecular Assemblies on Graphene

Qiaoyu Zhou^{a, ‡}, Yibao Li^{b, ‡}, Qiang Li^c, Yibing Wang^a, Yanlian Yang^a, Ying Fang^{a,*} and Chen Wang^{a,*}*Received (in XXX, XXX) Xth XXXXXXXXX 20XX, Accepted Xth XXXXXXXXX 20XX*

DOI: 10.1039/b000000x

We studied the self-assembly of trimesic acid on single- and few-layer graphene supported by SiO₂ substrates. A scanning tunneling microscope operated under ambient conditions was utilized to image supramolecular networks of trimesic acid at liquid-graphene interfaces. Trimesic acid can self-assemble into large-scale, highly ordered adlayers on graphene surfaces. Phase transition of trimesic acid adlayer from a close-packed structure to a porous chicken-wire structure was observed by changing from single- to few-layer graphene, which was attributed to the modulation of molecule-graphene interactions by the layer number of graphene. The guest-induced phase transition of trimesic acid by complexation with coronene on single-layer graphene further confirms that supramolecular networks on graphene can be rationally tailored with sub-nanometer resolution by balancing between intermolecular vs. molecule-graphene interactions. We further investigated effects of trimesic acid adlayers on electronic transport properties of graphene transistors. The adsorption of trimesic acid induces p-doping, and defects in the adlayers cause scattering of charge carriers in single-layer graphene.

Introduction

Graphene¹⁻³ has attracted tremendous research attention due to its unique physicochemical properties and potential applications. Many applications, including graphene based molecular devices and electrical/mechanical sensors, require the bare graphene surfaces to be engineered with additional functionalities.^{4,5} Thus the development of surface modification strategies is of practical importance for graphene devices. The adsorption and two-dimensional (2D) self-assembly of organic molecules on graphene surfaces have been proposed to create homogeneous and well-defined interfaces to graphene. In particular, initial progress has been made by supramolecular assembly of 3,4,9,10-perylene tetracarboxylicdianhydride (PTCDA) on epitaxial graphene (EGra) supported on silicon carbide (SiC) substrates.^{6,7} Submolecular characterization by scanning tunneling microscopy (STM) revealed that the supramolecular PTCDA network on EGra-SiC closely resembles that on highly-oriented-pyrolytic-graphite (HOPG) and is insensitive to defects or the layer number of EGra.⁶ Thus the self-assembly of PTCDA is mainly governed by strong intermolecular interactions between PTCDA molecules, instead of molecule-substrate interactions. STM studies of n-alkane derivatives on exfoliated graphene revealed the formation of long-range supramolecular networks, in which the lamellar configuration of the self-assembled molecules was also fastened by strong van der Waals interactions between long alkyl chains of molecules.⁸ On the other hand, switchable self-assemblies and their controlled response to external stimuli are among the most attractive routes to functional nanoscale structures in material

science,⁹⁻¹¹ and it can potentially open up new interests in engineering graphene based supramolecular devices.

A promising class of molecules to form switchable supramolecular structures employs directional hydrogen bond (H-bond) networks. The molecule 1,3,5-benzenetricarboxylic acid, or trimesic acid (TMA), has been shown to be an excellent building block of such kind (Fig. 1a). TMA is a planar molecule with a benzyl core that can interact with graphite or metal surfaces. The 3-fold-symmetrically carboxyl groups on TMA can self-associate through intermolecular H-bonds in either cyclic dimer- or trimer-configuration (Fig. 1b), which offers TMA self-assemblies structural and functional diversity.¹² Previous STM studies on HOPG substrates have reported two porous supramolecular networks of TMA, chicken-wire and flower structures,¹³ at solvent-HOPG interfaces under ambient conditions, and the phase transition between the two structures can be induced by solvent-induced polymorphism.¹⁴ Additionally, the self-assembly of TMA on Au (111) surfaces was also investigated by in-situ STM, and the supramolecular networks of TMA on Au (111) were found to be dependent on surface potentials of Au (111).^{15, 16} Such reports have demonstrated that the self-assembly of TMA can be regulated by external stimulation. Herein, by choosing TMA molecule as a model system, we report switchable supramolecular assemblies on graphene sheets and their effects on electronic properties of graphene field effect transistors (FETs).

Result and discussion

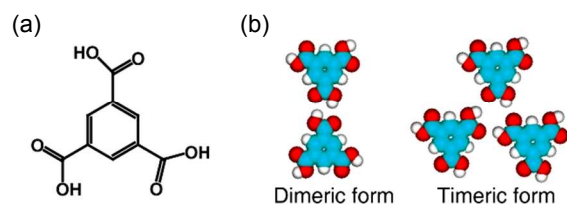


Fig. 1 TMA and its hydrogen bond motifs. (a) The chemical structure of TMA. (b) TMA hydrogen bond motif in dimeric and trimeric form, where blue, red, and white sphere represent C, O, and H atoms, respectively.

STM can directly resolve the molecular arrangements and has been successfully applied to study interactions in supramolecular structures. Previous reports mainly described graphene supported by metals (Cu or Ru) or SiC substrates, whereas graphene supported by an insulating SiO₂ substrate is currently the most relevant to nanoelectronics.^{17, 18} Here, mechanically exfoliated single- or few-layer graphene sheets were transferred onto insulating SiO₂ substrates, and their layer number was identified by Raman spectroscopy (Fig. S1†). A graphene sheet was then contacted to gold metal pads (20 mm × 20 mm squares) deposited by using a shadow-mask technique (Fig. S2a†).⁸ Since no resist or chemical was involved during fabrication, no contamination to the pristine graphene surfaces occurred. The gold pads were then

electrically connected to the STM sample holder and thus provided a return path of the tunneling current between graphene and the STM tip (Pt/Ir) (Fig. S2b†). To prepare TMA adlayers on graphene, 2 μL of 1 μM TMA in 1-octanoic acid was deposited on the graphene surfaces before STM characterization.¹⁶ We note that 1-octanoic acid is electrically nonconductive, and its vapor pressure at room temperature is low enough to allow STM characterization at the liquid-solid interface over hours. All STM images were recorded in the constant-current mode under ambient condition.

Fig. 2a is the STM image of a single-layer graphene sheet after deposition of TMA from 1-octanoic acid solution, which shows that TMA formed a well-ordered supramolecular network. The domains of the TMA adlayer can span over hundreds of nanometers on single-layer graphene, indicating the stability of the supramolecular structures at room temperature. Fig. 2b is a high resolution STM image, which shows that the TMA molecules form a close-packed structure on the single-layer graphene surface. A unit cell length of ~ 0.9 nm was measured for the TMA close-packed lattice, which agrees with the dimension of an individual TMA molecule flat-lying on the graphene sheet by π-π interaction. Therefore the close-packed configuration of the 2D network is associated with TMA self-assembling through the intermolecular formation of purely 3-fold hydrogen bonded motif. The proposed structural model derived from STM observations is presented in Fig. 2c.

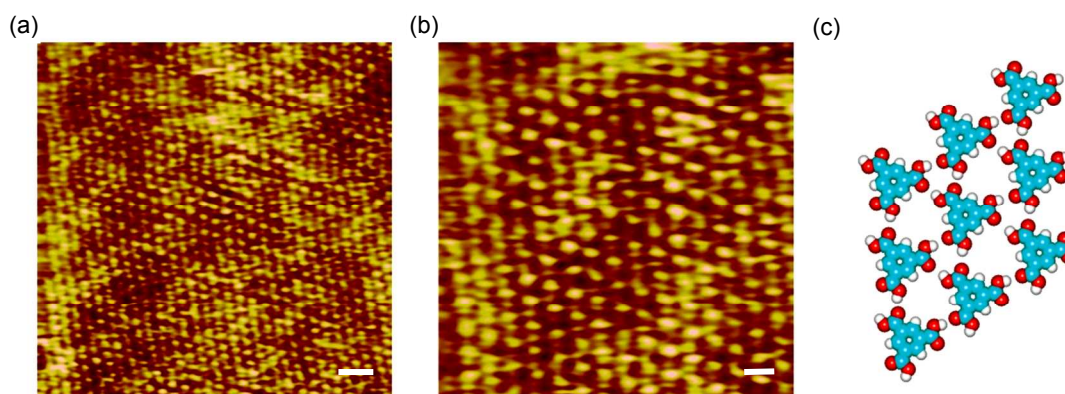


Fig. 2 Self-assembled TMA adlayer at the 1-octanoic acid/single-layer graphene interface. (a) Typical large-scale STM image of the TMA supramolecular network on single-layer graphene/SiO₂. STM image parameters: area = 50.6 nm × 50.6 nm, $V = 779.8$ mV, $I = 411.4$ pA. The scale bar is 5 nm. (b) High-resolution STM image of TMA supramolecular network on single-layer graphene/SiO₂. STM image parameters: area = 26.5 nm × 26.5 nm, $V = 779.8$ mV, $I = 411.4$ pA. The scale bar is 2 nm. (c) Molecular model of the TMA close-packed structure.

To our knowledge, the close-packed network of TMA has not been reported on HOPG surfaces at room-temperature. Previous studies have shown that the layer number of graphene can strongly affect the physicochemical properties and reactivity of graphene. For example, single-layer graphene was found to be 10 times more reactive to 4-nitrobenzene diazonium salt than bi- and few-layer graphene.¹⁹ Single-layer graphene deposited with silver (Ag) films also shows the largest SERS enhancement factor due to strong interactions between Ag and single-layer graphene.²⁰ Thus to account for the different TMA polymorphs on single-layer graphene and HOPG, we next investigated the dependence of TMA self-assemblies on the layer number of graphene in detail.

As shown in Fig. 3a and Fig. S3†, the coexistence of two different TMA self-assemblies was observed at 1-octanoic acid/bi-layer graphene interface. We note that, compared with single-layer graphene, bi-layer graphene shows reduced nanoscale surface corrugations, which thus facilitates high resolution STM imaging on bi-layer graphene (Fig. 3b and 3c). In domain I, a close packed structure of TMA was formed on the bi-layer graphene (Fig. 3b), resembling that on single-layer graphene. Each bright spot appears as an equilateral triangle and the intermolecular distance was measured to be approximately 1.0 nm, which is consistent with individual TMA molecules flat-lying with the benzyl ring parallel to bi-layer graphene. On the basis of above analysis, the corresponding molecular structure of

TMA in domain I is superimposed on the STM image in Fig. 3b.

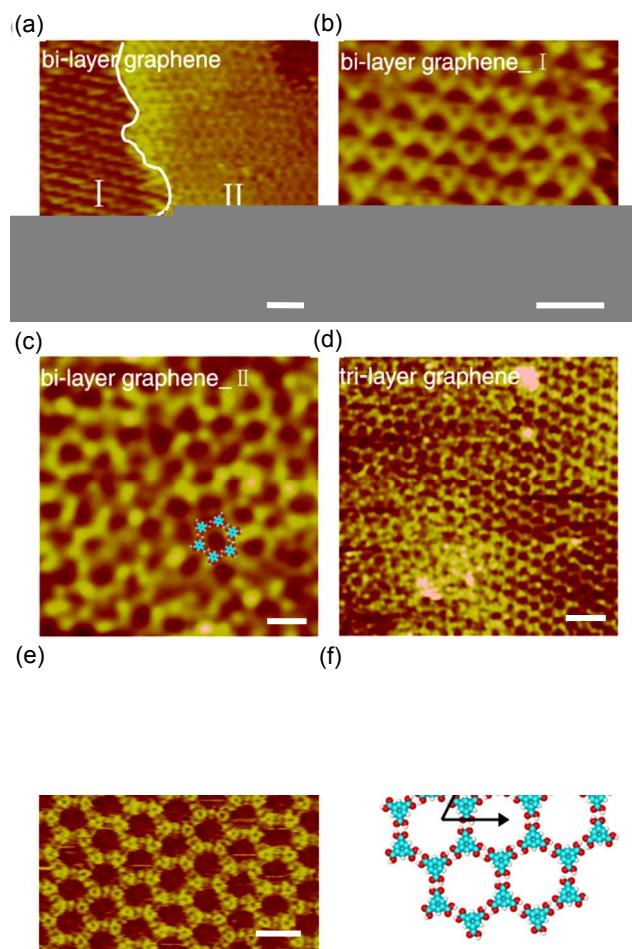


Fig. 3 Self-assembled TMA adlayers at 1-octanoic acid/few-layer graphene and 1-octanoic acid/graphite interfaces. (a) Large-scale STM image of TMA on bi-layer graphene/SiO₂. STM image parameters: area = 37.7 nm × 37.7 nm, V = 690.3 mV, I = 457.8 pA. The scale bar is 5 nm. (b) High-resolution STM image of TMA on bi-layer graphene/SiO₂ corresponding to domains I in (a). STM image parameters: area = 7.9 nm × 7.9 nm, V = 591.1 mV, I = 451.7 pA. The scale bar is 2 nm. (c) High-resolution STM image of TMA on bi-layer graphene/SiO₂ corresponding to domains II in (a). STM image parameters: area = 14.0 nm × 14.0 nm, V = 903.6 mV, I = 195.3 pA. The molecular models for the assembling structure are superimposed on the STM images of domains I (b) and II (c), respectively. The scale bar is 2 nm. (d) STM image of the TMA chicken-wire structure on tri-layer graphene/SiO₂. STM image parameters: area = 34.6 nm × 34.6 nm, V = 857.8 mV, I = 260.9 pA. The scale bar is 5 nm. (e) STM image of the TMA chicken-wire structure on HOPG. STM image parameters: area = 12.3 nm × 12.3 nm, V = 735.6 mV, I = 357.2 pA. The scale bar is 2 nm. (f) Molecular model for TMA chicken-wire structure, in which the two lattice vector lengths are both 1.7 nm and separated by an angle of 60°

In domain II on the bi-layer graphene, a porous chicken-wire structure of TMA was identified (Fig. 3c). As the thickness of graphene increases to tri-layers, only the chicken-wire structure of TMA adlayer was observed at the 1-octanoic acid/tri-layer graphene interface (Fig. 3d). Further, selective self-assembly of TMA in the chicken-wire structure was also observed at the 1-octanoic acid/HOPG interface (Fig. 3e and Fig. S4†), which is consistent with former reports¹⁴. The corresponding molecular model of the chicken-wire structure is presented in Fig. 3f. The

chicken-wire structure is composed of 6-fold rings of TMA molecules that self-assembly through purely 2-fold hydrogen bonded motif. The open pores of the chicken-wire network have a pore diameter of ~ 1.1 nm and a periodicity of ~ 1.7 nm, which thus results in a ~ 50% decrease of the surface molecular density than that of the close-packed TMA assembly. In the first approximation, the molecular coverage, or the packing efficiency, of different TMA polymorphs is proportional to the strength of the molecule-substrate interaction.²¹ Thus, the highest molecular density of TMA close-packed structure on single-layer graphene indicates the strongest molecule-substrate interaction between TMA and single-layer graphene. The origin for the observed different supramolecular structures on single- vs. multi-layer graphene might be a complex combination of dispersive and electrostatic interactions. Firstly, the band structure of single-layer graphene is distinctively different from those of multi-layered graphene. The electronic band structure of graphene has a linear dispersion near the K point. On the other hand, the coupling between the two graphene layers in a bi-layer graphene sheet leads to parabolic dispersion and a large density of state near band touching point.²² Secondly, former electrostatic force microscopy (EFM) measurements have shown that surface potentials increases with layer number of graphene,²³ which can result in different electrostatic interactions between TMA and graphene.

The use of a guest template to transform the structure of supramolecular networks has been recently demonstrated in 2D molecular systems.²⁴ We further investigated the possibility to transform TMA-graphene supramolecular structures with a guest molecule. Coronene (COR) was chosen as the guest molecule to complex with TMA. COR is a planar molecule consisting of seven interconnected benzene rings and has a diameter of ~ 1 nm. DFT simulation has shown that the incorporation of a coronene in the pore of a chicken-wire TMA hexagonal cell leads to an intermolecular energy gain of about -0.20 eV,²⁵ thus COR is expected to significantly enhance the stability of a TMA chicken-wire structure over other polymorphs. The good complementarity between COR and the pore of TMA chicken-wire polymorph has been experimentally demonstrated by the crystallization of their molecular complex (TMA)₂-COR.²⁶ Here we are interested in finding out whether coronene can stimulate the structural transition of TMA adlayers on single-layer graphene/SiO₂.

TMA and COR in 1-octanoic acid were sequentially added to the surfaces of single-layer graphene/SiO₂. STM images of the resulting adlayer structure at 1-octanoic acid/single-layer graphene interface were presented in Fig. 4, which reveals the formation a chicken-wire structure of TMA with COR sitting in the pores. Following addition of COR, no evidence of the close-packed TMA structure was observed at 1-octanoic acid/single-layer graphene interface. This efficient polymorphic transformation process occurs as a result of both hydrogen-bonding energy gain and the matching of size and shape between COR and the pore of TMA network (Fig. 4c). Thus it confirms our ability to rationally program graphene-based supramolecular structures by balancing between intermolecular and molecule-substrate interactions.

Cite this: DOI: 10.1039/c0xx00000x

www.rsc.org/xxxxxx

ARTICLE TYPE

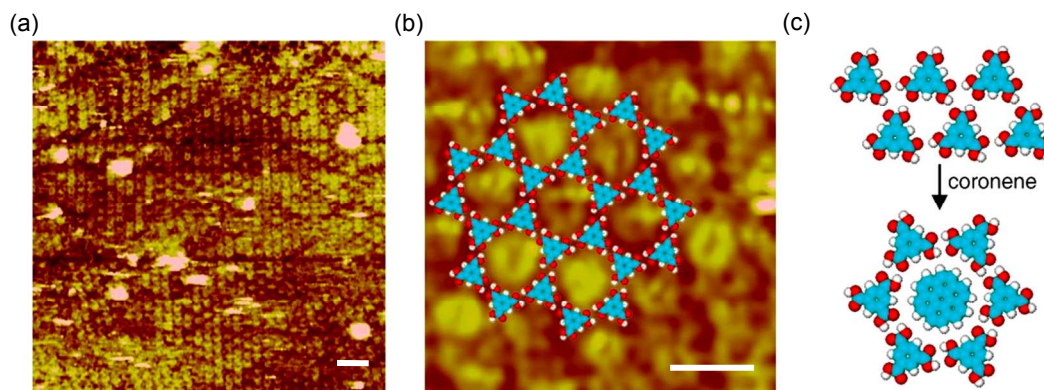


Fig. 4 Guest-induced structural transformation of TMA at the 1-octanoic acid/single-layer graphene interface. (a) Typical large-scale STM image of TMA-COR host-guest structure on single-layer graphene/SiO₂. STM image parameters: area = 56.2 nm × 56.2 nm, V = 1012.0 mV, I = 192.3 pA. The scale bar is 5 nm. (b) High-resolution STM image of TMA-COR hybrid assemblies on single-layer graphene/SiO₂. For clarity, the molecular structure of TMA is superimposed on the STM image. STM image parameters: area = 8.4 nm × 8.4 nm. The center-to-center distance of the pores is 1.7 nm and each pore is ~ 1.0 nm. The scale bar is 2 nm. (c) Proposed molecular mechanism for guest induced structural transformation from the close-packed to the chicken-wire structure of TMA by complexation with COR.

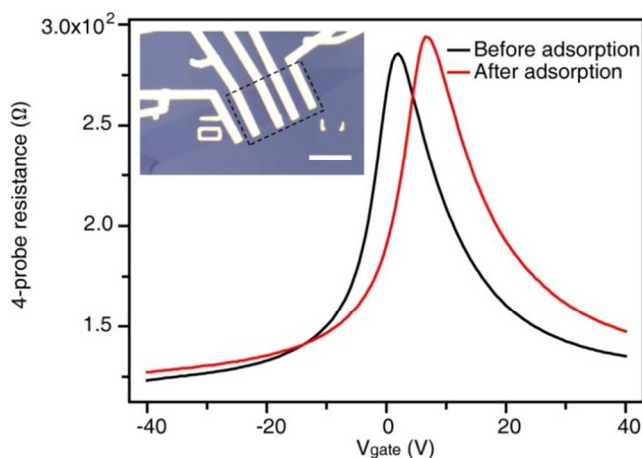


Fig. 5 Four-probe transfer curves of a GraFET before (black) and after adsorption (red) of the TMA adlayer, respectively. The black curve shows the current of the GraFET plotted against the applied back-gate voltage after overnight incubation of the device chip in 1-octanoic acid. The red curve was measured for the same device after incubation in 1 μM TMA in 1-octanoic acid for 2 hours. Inset, optical picture of the device. Scale bar, 10 μm.

We have shown that self-assembled supramolecular networks on graphene can be rationally tailored with sub-nanometer resolution, which may provide new opportunities for graphene-based electronics. However, electronic interactions between the adlayer and graphene transistors have yet to be elucidated. Next, we investigated the effects of the self-assembled TMA adlayer on transport properties of single-layer graphene transistors. GraFETs in four-probe configurations were fabricated on Si/SiO₂ substrates by electron beam lithography and subsequent formation of 3 nm Cr/30 nm Au metal contacts.⁸ Four-probe electrical measurements of GraFETs were performed in a home-made PDMS chamber filled with 1-octanoic acid solution, and all

devices were back-gated through 285 nm SiO₂. Fig. 5 shows a representative conductance versus back-gate voltage characteristics of a single-layer graphene transistor before and after adsorption of the TMA adlayer. Firstly, Dirac points, corresponding to the overall charge neutrality point, of ten single-layer graphene devices shifted positively ($\Delta V_{DP} = (4.5 \pm 0.7)$ V) after the adsorption of TMA (Fig. S5†), which shows that the TMA adlayer induces p-type doping in single-layer graphene. The doping density in single-layer graphene by the TMA adlayer can be calculated as $n_{\text{doping}} = (\Delta V_{DP} \times C)/e$, where C is the gate capacitance and e is the electron charge. The averaged ΔV_{DP} by the TMA adlayer thus gives a doping density of 3×10^{11} cm⁻² in single-layer graphene, corresponding to 0.003e by each TMA molecule. Secondly, in the linear regions of conductance vs. back-gate voltage characteristics, the mobility of the GraFET decreased from 5000 to 3500 cm²/Vs for hole- and 4300 to 3000 cm²/Vs for electron-carriers, respectively, after the adsorption of TMA adlayer. We attribute the reduced mobility in single-layer graphene to the scattering effects by impurities in the TMA adlayer.²⁷ The impurity centers are formed at defects in the TMA adlayer, such as point defects or boundaries between rotated TMA domains.

Conclusions

In conclusion, we have demonstrated that graphene-based supramolecular structures can be rationally designed by balancing between intermolecular vs. molecule-substrate interactions. The guest-host network on single-layer graphene provides a strategy for fixing single molecules, with sub-nanometer resolution, on graphene, which can be an attractive route in the development of molecular-level mechanical or electronic graphene devices.

Method

Sample preparations

Single-layer graphene flakes for scanning tunneling microscopy (STM) imaging were contacted to 3 nm Cr/15 nm Au by thermal evaporation using a shadow-mask cut from aluminum foils. Self-assembly of 1-octadecanethiol molecules on graphene was prepared before STM imaging. 1-octanoic acid and trimesic acid (TMA) were purchased from Sigma-Aldrich and used as received. The assemblies of TMA or TMA-coronene were prepared by their 1 μ M solutions deposited on graphene.

Graphene field effect transistors (Gra-FETs) were fabricated by e-beam lithography on PMMA950 A4 (MicroChem Inc.) using a SEM/FIB dual-beam instrument (Nova 200 NanoLab, FEI) interfaced with an Elphy Quantum software (Raith Company). Metallization was subsequently carried out by thermal evaporation of 5 nm Cr/50 nm Au/3 nm Cr. After lift-off of the resist, chips with Gra-FETs were annealed at 300°C for 3 hours under a vacuum of $\sim 10^{-5}$ torr (TPS-Compact pump, Varian) to strip the resist contamination from graphene surfaces.

Characterization

Raman details

The Graphene flakes were deposited by mechanical exfoliation of natural graphite using 3M scotch tapes. Silicon wafers with 285 nm thermal oxide were purchased from Silicon Valley Microelectronics, Inc.. A micro-Raman spectroscopy (Renishaw Via Raman Spectroscope) was used to confirm the layer number of graphene, and the wavelength and power of the laser were set as 514 nm and 1.0 mW.

STM details

STM measurements were performed under ambient conditions at room temperature with a Nanoscope IIIA SPM system (Digital Instruments, Santa Barbara, CA). The tips were mechanically formed from Pt/Ir wires (90/10). All STM image were acquired in constant current mode, and typical tunneling conditions are set point: 0.3 nA, bias: 0.65 V. The tip was grounded, and no gate voltage was applied during STM imaging.

Transport details

Transport properties of graphene sensors were characterized using a semiconductor parameter analyzer (Keithley 4200, Keithley Co. Ltd.) at room temperature. A 3 μ A current was applied in DC mode, and the voltage between the two inner electrodes was monitored as a function of the back gate voltage applied through 285 nm SiO₂.

Acknowledgement

This work was supported by the National Natural Science Foundation of China ((21322302, 21303024, and 21365003).

Notes and references

^a National Center for Nanoscience and Technology, China, 11 Beiyitiao Street, Zhongguancun, Beijing 100190. E-mail: Fangy@nanoctr.cn; Wangch@nanoctr.cn.

^b Key Laboratory of Organo-pharmaceutical Chemistry, Gannan Normal University, Ganzhou 341000, P. R. China.

^c Interdisciplinary Nanoscience Center (iNANO), Aarhus University, Gustav Wieds Vej 14, 8000 Aarhus C, Denmark

† Electronic Supplementary Information (ESI) available: [details of any supplementary information available should be included here]. See DOI: 10.1039/b000000x/

‡ These authors contributed equally to this work.

- 1 K. S. Novoselov, A. K. Geim, S. V. Morozov, D. Jiang, Y. Zhang, S. V. Dubonos, I. V. Grigorieva and A. A. Firsov, *Science*, 2004, **306**, 666.
- 2 Y. B. Zhang, Y. W. Tan, H. L. Stormer and P. Kim, *Nature*, 2005, **438**, 201.
- 3 F. Schedin, A. K. Geim, S. V. Morozov, E. W. Hill, P. Blake, M. I. Katsnelson and K. S. Novoselov, *Nat. Mater.*, 2007, **6**, 652.
- 4 Y. Shao, J. Wang, H. Wu, J. Liu, I. A. Aksay and Y. Lin, *Electroanalysis*, 2010, **22**, 1027.
- 5 Y. Ohno, K. Maehashi and K. Matsumoto, *J. Am. Chem. Soc.*, 2010, **132**, 18012.
- 6 Q. H. Wang and M. C. Hersam, *Nat. Chem.*, 2009, **1**, 206.
- 7 H. Huang, S. Chen, X. Gao, W. Chen and A. T. S. Wee, *ACS Nano*, 2009, **3**, 3431.
- 8 T. Zhang, Z. Cheng, Y. Wang, Z. Li, C. Wang, Y. Li and Y. Fang, *Nano Lett.*, 2010, **10**, 4738.
- 9 M. Alemani, M. V. Peters, S. Hecht, K.-H. Rieder, F. Moresco and L. Grill, *J. Am. Chem. Soc.*, 2006, **128**, 14446.
- 10 M. Ruben, D. Payer, A. Landa, A. Comisso, C. Gattinoni, N. Lin, J.-P. Collin, J.-P. Sauvage, A. De Vita and K. Kern, *J. Am. Chem. Soc.*, 2006, **128**, 15644.
- 11 Y. L. Yang, Q. L. Chan, X. J. Ma, K. Deng, Y. T. Shen, X. Z. Feng and C. Wang, *Angew. Chem. Inter. Ed.*, 2006, **45**, 6889.
- 12 Y. Ye, W. Sun, Y. Wang, X. Shao, X. Xu, F. Cheng, J. Li and K. Wu, *J. Phys. Chem. C*, 2007, **111**, 10138.
- 13 S. Griessl, M. Lackinger, M. Edelwirth, M. Hietschold and W. M. Heckl, *Single Mol.*, 2002, **3**, 25.
- 14 M. Lackinger, S. Griessl, W. M. Heckl, M. Hietschold and G. W. Flynn, *Langmuir*, 2005, **21**, 4984.
- 15 Y. Ishikawa, A. Ohira, M. Sakata, C. Hirayama and M. Kunitake, *Chem. Commun.*, 2002, **22**, 2652.
- 16 G. J. Su, H. M. Zhang, L. J. Wan, C. L. Bai and T. Wandlowski, *J. Phys. Chem. B*, 2004, **108**, 1931.
- 17 E. Stolyarova, K. T. Rim, S. Ryu, J. Maultzsch, P. Kim, L. E. Brus, T. F. Heinz, M. S. Hybertsen and G. W. Flynn, *P. Nat. Acad. Sci. U. S. A.*, 2007, **104**, 9209.
- 18 M. Ishigami, J. H. Chen, W. G. Cullen, M. S. Fuhrer and E. D. Williams, *Nano Lett.*, 2007, **7**, 1643.
- 19 R. Sharma, J. H. Baik, C. J. Perera and M. S. Strano, *Nano Lett.*, 2010, **10**, 398.
- 20 J. Lee, K. S. Novoselov and H. S. Shin, *ACS Nano*, 2011, **5**, 608.
- 21 J. M. MacLeod, O. Ivasenko, C. Fu, T. Taerum, F. Rosei and D. F. Perepichka, *J. Am. Chem. Soc.*, 2009, **131**, 16844.
- 22 E. Mccan, V. I. Fal'ko, *Phys. Rev. Lett.*, 2006, **96**, 086805.
- 23 S. H. Zhao, Y. Lv, X. J. Yang, *Nanoscale Res. Lett.*, 2011, **6**, 498.
- 24 S. Furukawa, K. Tahara, F. C. De Schryver, M. Van der Auweraer, Y. Tobe and S. De Feyter, *Angew. Chem. Inter. Ed.*, 2007, **46**, 2831.
- 25 M. Blunt, X. Lin, M. d. C. Gimenez-Lopez, M. Schroder, N. R. Champness and P. H. Beton, *Chem. Commun.*, 2008, **0**, 2304.
- 26 O. Ermer and J. Neudörfl, *Helv. Chim. Acta*, 2001, **84**, 1268.
- 27 A. A. Balandin, *Nat. Nanotechnol.*, 2013, **8**, 549.